

A Comparative Study of Molecular Dynamics in Cartesian and in Internal Coordinates: Dynamical Instability in the Latter Caused by Nonlinearity of the Equations of Motion

SANG-HO LEE, KIM PALMO, SAMUEL KRIMM

Biophysics Research Division and Department of Physics, University of Michigan,
930 N. University Ave., Ann Arbor, Michigan 48109

Received 18 July 2006; Accepted 13 November 2006

DOI 10.1002/jcc.20627

Published online 5 February 2007 in Wiley InterScience (www.interscience.wiley.com).

Abstract: The stability of a general molecular dynamics (MD) integration scheme is examined for simulations in generalized (internal plus external) coordinates (GCs). An analytic expression is derived for the local error in energy during each integration time step. This shows that the explicit dependence of the mass-matrix on GCs, which makes the system's Lagrange equations of motion nonlinear, causes MD simulations in GCs to be less stable than those in Cartesian coordinates (CCs). In terms of CCs, the corresponding mass-matrix depends only on atomic masses and thus atomistic motion is subject to the linear Newton equations, which makes the system more stable. Also investigated are two MD methods in GCs that utilize nonzero elements of the vibrational spectroscopic B-matrices. One updates positions and velocities in GCs that are iteratively adjusted so as to conform to the velocity Verlet equivalent in GCs. The other updates positions in GCs and velocities in CCs that are adjusted to satisfy the internal constraints of the new constrained WIGGLE MD scheme. The proposed methods are applied to an isolated *n*-octane molecule and their performances are compared with those of several CCMD schemes. The simulation results are found to be consistent with the analytic stability analysis. Finally, a method is presented for computing nonzero elements of B-matrices for external rotations without imposing the Casimir–Eckart conditions.

© 2007 Wiley Periodicals, Inc. J Comput Chem 28: 1107–1118, 2007

Key words: molecular dynamics; internal coordinate; external rotation; constrained dynamics; numerical integration

Introduction

Information on the structures and dynamics of biomolecules (e.g., proteins, DNA, and RNA) is basic to an understanding of their biological properties. As a standard coordinate system, Cartesian coordinates (CCs) have been used to visualize detailed atomic level structures and motions. However, molecular internal coordinates (ICs: bond lengths, bond angles, in-plane/out-of-plane wags, or torsion angles) have also been efficiently used in such areas as vibrational (infrared and Raman) normal mode analyses,^{1–3} molecular mechanics (MM) conformation energy analyses,^{4–6} Monte Carlo (MC) simulations,^{7–15} *ab initio* geometry optimizations,^{16–30} quantum MC simulations,^{31,32} and molecular docking problems.^{33–37} This is because intramolecular interaction energy terms, as well as molecular internal vibrations, are easily described in ICs. However, in contrast to the linearity of the Newton equations of motion in CCs, the classical molecular dynamics (MD) equations to be solved in ICs are not only nonlinear but also demand nontrivial computation processes at each numerical integration step. Thus, MD simulations in ICs have not been as popular as those in CCs.

The equations of motion for typical MD simulations are not analytically solvable, and therefore they are solved approximately by a numerical integration method. To maintain the system's stability, the integration time step routinely has to be kept small enough (less than 1 fs) to resolve such fast motions as vibrations of bond length ICs. This imposes a serious limitation on routine simulations in a longer time range than ns, where interesting biomolecular conformation changes may take place. However, the fast atomistic motions related to most bond stretching and angle bending vibrations are localized^{1–3} and, during certain simulation time ranges of a molecule, the average changes in the internal bond lengths and bond angles are negligible compared with those in torsion (viz., dihedral) angles.³⁸ Thus, freezing (or constraining) all bond length coordinates enables one to use a time step larger than that for an unconstrained CCMD simulation.^{39,40} On the other hand, in the early studies

Correspondence to: S. Krimm; e-mail: skrimm@umich.edu

Contract/grant sponsor: NSF; contract/grant number: MCB-0212232 and DMR-0239417

of conformation energies and dynamics models in ICs, molecules were treated as chains of linked rigid bodies with/without constraints on bond lengths or bond angles.^{41–45} (Interestingly, similar ideas can also be found in mechanical dynamics treatments of complex spacecraft.^{46,47}) In this approach, since changes in torsion ICs dominate conformational changes, energy minimizations for biomolecules are efficiently carried out first in a space of torsion degrees of freedom and then other ICs are included in a further calculation. This idea has been developed into the torsion angle (or reduced variable) MD method,^{48–55} where all internal degrees of freedom except for torsions are simply neglected. It was further developed to include bond lengths and bond angles,^{56–60} to incorporate quaternion parameters and angular velocities for rotations of linked rigid body subunits,^{61,62} or to adopt the fast recursive algorithm for mechanical models of linked rigid bodies or hinges.^{63–74} In addition to successful applications to structural calculations,^{67,69,71,74–81} reports of using increased integration time steps greater than 4 fs^{52,68,72,73} have made the ICMD method very attractive.

In this development, and based on the spectroscopic B-matrix (viz., the transformation matrix from quantities in CCs to those in ICs),^{1,2} we have also introduced an ICMD scheme.^{82,83} The efficiency of this scheme lies in the fact that inversion of the large mass-matrix in solving the nonlinear equations of motion is indirectly accomplished by computing the sparse B-matrix elements, which are nonzero only for a few (at most four) related atoms for each IC. In this article, we report a further refinement of the B-matrix ICMD method based on WIGGLE (a new constrained CCMD scheme),⁸⁴ the velocity update in CCs by Pulay and Paizs,⁸⁵ and an improved computation of B-matrix elements for external rotations [see Appendix]. The method is applied to an isolated octane molecule, and its performance (with/without constraints on internal bond lengths) is compared with that of the CCMD method. Mazur made detailed comparative studies between ICMD and CCMD simulations,^{60,86} and found no essential differences between the two MD trajectories. However, we have found that the ICMD method is inherently an order of the integration time step less stable than the CCMD method with/without internal constraints. This is consistent with our detailed theoretical analysis of the two dynamic stabilities. Our derived analytic expression for energy drift in each integration time step is also consistent with that of Gibson and Scheraga.⁵² Overall, this result indicates that, for the purpose of MD simulation itself, CCs are to be preferred to ICs with/without internal constraints.⁸⁷

In Dynamical Equations of Motion in ICs with Internal Constraints, equations of motion in generalized (internal plus external) coordinates (GCs) with internal constraints are introduced. In Local Energy Drift, to analyze the stability of a general ICMD scheme, we investigate the extent to which the system conserves its total energy in an integration time step. In ICMD Algorithms, we introduce two optimal constrained ICMD schemes: AICMD adopts an iterative treatment to conform to the velocity Verlet⁸⁸ equivalent in GCs, and BICMD incorporates the velocity update in CCs⁸⁵ based on WIGGLE.⁸⁴ In Application to an *n*-Octane Molecule, the two schemes are applied to an isolated octane molecule and their results are compared with those from several CCMD methods with/without con-

straints on all CH bond lengths. Finally, an improved method of computing nonzero B-matrix elements for external rotations is presented in the Appendix.

Dynamical Equations of Motion in ICs with Internal Constraints

Without a loss of generality, we consider an isolated molecule of *p* atoms whose masses and Cartesian positions are given by m_λ and \mathbf{x}_λ ($\lambda = 1, \dots, p$), respectively. We define $\mathbf{X} \equiv (x_1^1 x_1^2 x_1^3 \dots x_p^1 x_p^2 x_p^3)^T$, with superscript *T* representing the transpose of a matrix. Let \mathbf{S} be a nonredundant set of GCs such that, in the neighborhood of an arbitrary molecular configuration \mathbf{S}_{ec} (expansion center),

$$\mathbf{S} = \mathbf{S}_{\text{ec}} + \mathbf{B}\Delta\mathbf{X} + \frac{1}{2}\Delta\mathbf{X}^T\mathbf{B}_2\Delta\mathbf{X} + \dots \quad (1)$$

$$\mathbf{X} = \mathbf{X}_{\text{ec}} + \mathbf{A}\Delta\mathbf{S} + \frac{1}{2}\Delta\mathbf{S}^T\mathbf{A}_2\Delta\mathbf{S} + \dots, \quad (2)$$

with $\Delta\mathbf{S} \equiv \mathbf{S} - \mathbf{S}_{\text{ec}}$, $\Delta\mathbf{X} \equiv \mathbf{X} - \mathbf{X}_{\text{ec}}$, $\mathbf{B} \equiv [\partial\mathbf{S}/\partial\mathbf{X}]_{\text{ec}} \equiv [\partial\mathbf{X}\mathbf{S}]_{\text{ec}}$, $\mathbf{B}_2 \equiv [\partial_{\mathbf{X}}\partial_{\mathbf{X}}\mathbf{S}]_{\text{ec}} \equiv [\partial_{\mathbf{X}}^2\mathbf{S}]_{\text{ec}}$, $\mathbf{A} \equiv [\partial\mathbf{S}\mathbf{X}]_{\text{ec}}$, $\mathbf{A}_2 \equiv [\partial_{\mathbf{S}}^2\mathbf{X}]_{\text{ec}}$, and

$$\mathbf{A}\mathbf{B} = \mathbf{1} = \mathbf{B}\mathbf{A} \left(\sum_{\beta} A_{\beta}^{\nu} B_{\lambda k}^{\beta} = \delta_{\lambda}^{\nu} \delta_k^j \text{ and } \delta_{\gamma}^{\beta} = \sum_{\nu=1}^p \sum_{j=1}^3 B_{\nu j}^{\beta} A_{\nu}^{\gamma} \right). \quad (3)$$

Differentiating eq. (3), we have

$$\mathbf{B}^T\mathbf{A}_2\mathbf{B} + \mathbf{A}\mathbf{B}_2 = \mathbf{0} = \mathbf{A}^T\mathbf{B}_2\mathbf{A} + \mathbf{B}\mathbf{A}_2. \quad (4)$$

In using this simplified expression, we have to keep in mind that \mathbf{B}_2 and \mathbf{A}_2 are not regular matrices but third rank tensors. The expressions with specific tensor components corresponding to eq. (4) can be obtained by considering the expressions in the parenthesis of eq. (3). Thus, eqs. (1) and (2) are inverse relations to each other if eqs. (3) and (4) are satisfied. Specific methods of computing elements of \mathbf{B} , \mathbf{B}_2 , \mathbf{A} , and \mathbf{A}_2 can be found elsewhere.^{1,2,48,53,56,82,83,89} We have verified the correctness of analytical formulas for nonzero elements of \mathbf{B} and \mathbf{B}_2 by comparing results from numerical and analytical differentiations.

The system's classical kinetic energy *T* is now expressed by

$$2T = \dot{\mathbf{X}}^T \mathbf{m} \dot{\mathbf{X}} = \dot{\mathbf{S}}^T \mathbf{g} \dot{\mathbf{S}} \quad (5)$$

where a dot represents differentiation with respect to time and $\mathbf{g} \equiv \mathbf{A}^T \mathbf{m} \mathbf{A}$ is the mass-matrix, with \mathbf{m} being a $3p \times 3p$ diagonal matrix containing triads of atomic masses m_λ . In the presence of N_c nonredundant internal constraints $\sigma^\alpha(\mathbf{X}) = C^\alpha$ (constant) ($\alpha = 1, \dots, N_c$), which are represented by

$$\sigma(\mathbf{X}) = \mathbf{C}, \quad (6)$$

classical atomic motion is subject to the constrained potential energy

$$V_c \equiv V + \boldsymbol{\sigma}^T \boldsymbol{\Lambda} \quad (7)$$

where V is the system's potential energy without constraints and $\boldsymbol{\Lambda}$ is a column vector of the Lagrange undetermined parameters related to the constraint forces. Assuming V_c is not an explicit function of time and atomic velocities, the classical equations of motion in CCs are found to be

$$\mathbf{m}\ddot{\mathbf{X}} = -\partial_{\mathbf{X}}V_c = \mathbf{F}_X - \mathbf{B}_c^T \boldsymbol{\Lambda} \quad (8)$$

with $\mathbf{F}_X \equiv -\partial_{\mathbf{X}}V$ and $\mathbf{B}_c \equiv \partial\boldsymbol{\sigma}/\partial\mathbf{X} \equiv \partial_{\mathbf{X}}\boldsymbol{\sigma}$. Dynamic equations of motion without constraints are simply obtained by setting $\boldsymbol{\Lambda} = \mathbf{0}$. Successive differentiations of eq. (6) with respect to time provide additional equations for constraints:

$$\dot{\boldsymbol{\sigma}} = \mathbf{B}_c \dot{\mathbf{X}} = \mathbf{0} \quad (9)$$

$$\ddot{\boldsymbol{\sigma}} = \mathbf{B}_c \ddot{\mathbf{X}} + \dot{\mathbf{X}}^T \mathbf{B}_{2c} \dot{\mathbf{X}} = \mathbf{0} \quad (10)$$

with $\mathbf{B}_{2c} \equiv \partial_{\mathbf{X}}\mathbf{B}_c \equiv \partial_{\dot{\mathbf{X}}}^2\boldsymbol{\sigma}$. By using eqs. (8) and (10), for given $\dot{\mathbf{X}}$ and \mathbf{F}_X , the parameters $\boldsymbol{\Lambda}$ can be determined by solving

$$\mathbf{G}_{cc}\boldsymbol{\Lambda} = \mathbf{B}_c\mathbf{m}^{-1}\mathbf{F}_X + \dot{\mathbf{X}}^T \mathbf{B}_{2c}\dot{\mathbf{X}}, \quad (11)$$

where $\mathbf{G}_{cc} \equiv \mathbf{B}_c\mathbf{m}^{-1}\mathbf{B}_c^T$, with superscript -1 representing the inverse of a nonsingular matrix. In terms of the GCs, the Euler-Lagrange equations of motion are found to be

$$\mathbf{g}\ddot{\mathbf{S}} + \dot{\mathbf{S}}^T [\mathbf{A}^T \mathbf{m} \mathbf{A}_2] \dot{\mathbf{S}} + \partial_{\mathbf{S}}V_c = \mathbf{0}, \quad (12)$$

with the simplified second term being defined by

$$\dot{\mathbf{S}}^T [\mathbf{A}^T \mathbf{m} \mathbf{A}_2] \dot{\mathbf{S}} \equiv [\mathbf{A}^T \mathbf{m} (\dot{\mathbf{S}}^T \partial_{\mathbf{S}}) \mathbf{A}] \dot{\mathbf{S}} = \frac{1}{2} [(\dot{\mathbf{S}}^T \partial_{\mathbf{S}}) \mathbf{g}] \dot{\mathbf{S}}. \quad (13)$$

Dynamics trajectory information can be obtained from solving eq. (12). For systems of polyatomic molecules, this is done by numerical integration with a finite time step.

As a way of increasing the time step in MD simulations, it has been common to constrain such fast moving degrees of freedom as bond length ICs.^{39,40} We consider constraining some coordinates of \mathbf{S} so that \mathbf{S} can be separated into an unconstrained part \mathbf{S}_u and a constrained one $\mathbf{S}_c = \boldsymbol{\sigma}$, with $\mathbf{S}^T = (\mathbf{S}_u^T \mathbf{S}_c^T)$. In this case, it should be emphasized that the matrix \mathbf{g} in eq. (12) is still nonsingular and its inverse is well defined by $\mathbf{G} \equiv \mathbf{B}\mathbf{m}^{-1}\mathbf{B}^T$, so long as the whole \mathbf{S} is nonredundant, as we have already assumed. For a given molecular geometry, it is not difficult to find a desired nonredundant set \mathbf{S} of GCs. Thus, applying \mathbf{G} to the left-hand side of eq. (12), we obtain

$$\begin{aligned} \ddot{\mathbf{S}} &= -\dot{\mathbf{S}}^T [\mathbf{B} \mathbf{A}_2] \dot{\mathbf{S}} - \mathbf{B}\mathbf{m}^{-1} \partial_{\mathbf{X}}V_c \\ &= \dot{\mathbf{S}}^T \mathbf{A}^T [\mathbf{B}_2] \mathbf{A} \dot{\mathbf{S}} + \mathbf{B}\ddot{\mathbf{X}} \quad [\text{from eqs. (4) and (8)}] \\ &= \dot{\mathbf{X}}^T [\mathbf{B}_2] \dot{\mathbf{X}} + \mathbf{B}\ddot{\mathbf{X}}, \quad (14) \end{aligned}$$

which is the very expression obtainable from the second derivative of eq. (1) with respect to time.⁸⁵ For the constrained coordinates \mathbf{S}_c , this becomes an equation for $\boldsymbol{\Lambda}$ that is equivalent to eq. (11).

Local Energy Drift

The reliability of long time simulations of a dynamical system depends on the stability of the numerical integration scheme. The local error in total energy in each integration time step eventually affects the global stability, the latter depending on whether the local errors are cumulative or not. To determine the factors that affect the local energy drift, we consider the following general numerical integration scheme in GCs:

$$\mathbf{S}(\Delta t) = \mathbf{S}(0) + \Delta t \alpha \dot{\mathbf{S}}(0) + \Delta t^2 \{ \beta \ddot{\mathbf{S}}(0) + \gamma \ddot{\mathbf{S}}(\Delta t) \} \quad (15)$$

$$\dot{\mathbf{S}}(\Delta t) = \dot{\mathbf{S}}(0) + \Delta t \{ \varepsilon \ddot{\mathbf{S}}(0) + \omega \ddot{\mathbf{S}}(\Delta t) \}, \quad (16)$$

where $\alpha, \beta, \gamma, \varepsilon$, and ω are appropriate constants and variables $\mathbf{S}, \dot{\mathbf{S}},$ and $\ddot{\mathbf{S}}$ are assumed to satisfy eqs. (9)–(12) at each time step with suitable constraint parameters $\boldsymbol{\Lambda}$. In view of eq. (15), we can expand $\ddot{\mathbf{S}}(\Delta t)$ as

$$\ddot{\mathbf{S}}(\Delta t) = \ddot{\mathbf{S}}(0) + \Delta t \alpha [(\dot{\mathbf{S}}^T \partial_{\mathbf{S}}) \ddot{\mathbf{S}}](0) + \dots, \quad (17)$$

rewriting eqs. (15) and (16), respectively, by

$$\begin{aligned} \mathbf{S}(\Delta t) &= \mathbf{S}(0) + \Delta t \alpha \dot{\mathbf{S}}(0) + \Delta t^2 (\beta + \gamma) \ddot{\mathbf{S}}(0) \\ &\quad + \Delta t^3 \alpha \gamma [(\dot{\mathbf{S}}^T \partial_{\mathbf{S}}) \ddot{\mathbf{S}}](0) + \dots \quad (18) \end{aligned}$$

$$\begin{aligned} \dot{\mathbf{S}}(\Delta t) &= \dot{\mathbf{S}}(0) + \Delta t (\varepsilon + \omega) \ddot{\mathbf{S}}(0) \\ &\quad + \Delta t^2 \alpha \omega [(\dot{\mathbf{S}}^T \partial_{\mathbf{S}}) \ddot{\mathbf{S}}](0) + \dots \quad (19) \end{aligned}$$

Then, the total potential energy of eq. (7) at $\mathbf{S}(\Delta t)$ is Taylor expanded as

$$\begin{aligned} V_c(\Delta t) &= V_c(0) + \Delta t \alpha [(\dot{\mathbf{S}}^T \partial_{\mathbf{S}}) V_c](0) + \frac{\Delta t^2}{2} [2(\beta + \gamma) (\dot{\mathbf{S}}^T \partial_{\mathbf{S}}) V_c \\ &\quad + \alpha^2 \dot{\mathbf{S}}^T (\partial_{\mathbf{S}}^2 V_c) \dot{\mathbf{S}}](0) + O(\Delta t^3). \quad (20) \end{aligned}$$

The matrix $\mathbf{g}(\Delta t)$ is also expanded by the same form as this with each V_c being replaced by \mathbf{g} . Considering eq. (19), we can expand the kinetic energy of eq. (5) by

$$\begin{aligned}
T(\Delta t) = & T(0) + \Delta t \dot{\mathbf{S}}^T(0) \left[(\varepsilon + \omega) \mathbf{g} \ddot{\mathbf{S}} + \frac{\alpha}{2} \{ (\dot{\mathbf{S}}^T \partial_{\mathbf{S}}) \mathbf{g} \} \dot{\mathbf{S}} \right] (0) \\
& + \frac{\Delta t^2}{2} \left[(\varepsilon + \omega)^2 \ddot{\mathbf{S}}^T \mathbf{g} \ddot{\mathbf{S}} + 2\alpha\omega \dot{\mathbf{S}}^T \mathbf{g} \{ (\dot{\mathbf{S}}^T \partial_{\mathbf{S}}) \ddot{\mathbf{S}} \} \right. \\
& + (\beta + \gamma) \dot{\mathbf{S}}^T \{ (\ddot{\mathbf{S}}^T \partial_{\mathbf{S}}) \mathbf{g} \} \dot{\mathbf{S}} + 2\alpha(\varepsilon + \omega) \ddot{\mathbf{S}}^T \{ (\dot{\mathbf{S}}^T \partial_{\mathbf{S}}) \mathbf{g} \} \dot{\mathbf{S}} \\
& \left. + \frac{\alpha^2}{2} \dot{\mathbf{S}}^T \{ \dot{\mathbf{S}}^T (\partial_{\mathbf{S}}^2 \mathbf{g}) \dot{\mathbf{S}} \} \dot{\mathbf{S}} \right] (0) + O(\Delta t^3). \quad (21)
\end{aligned}$$

Similarly, the system's total energy, $E \equiv T + V_c$, at $\mathbf{S}(\Delta t)$ can be Taylor expanded by

$$E(\Delta t) = E(0) + \Delta t E^{(1)}(0) + \frac{\Delta t^2}{2} E^{(2)}(0) + \frac{\Delta t^3}{6} E^{(3)}(0) + \dots \quad (22)$$

By using eqs. (20) and (21), the coefficient $E^{(1)}$ is found to be

$$E^{(1)} = \dot{\mathbf{S}}^T \left\{ (\varepsilon + \omega) \mathbf{g} \ddot{\mathbf{S}} + \alpha \partial_{\mathbf{S}} V_c + \frac{\alpha}{2} [(\dot{\mathbf{S}}^T \partial_{\mathbf{S}}) \mathbf{g}] \dot{\mathbf{S}} \right\}. \quad (23)$$

If $\alpha = \varepsilon + \omega$, this term becomes zero from eqs. (12) and (13). Assuming this and arranging terms of Δt^2 with eq. (12), we obtain

$$\begin{aligned}
E^{(2)} = & (2\beta + 2\gamma - \alpha^2) \ddot{\mathbf{S}}^T \partial_{\mathbf{S}} V_c + \left(\beta + \gamma + \frac{1}{2} \alpha^2 \right) \dot{\mathbf{S}}^T [(\ddot{\mathbf{S}}^T \partial_{\mathbf{S}}) \mathbf{g}] \dot{\mathbf{S}} \\
& + \alpha(2\omega - \alpha) \dot{\mathbf{S}}^T \mathbf{g} [(\dot{\mathbf{S}}^T \partial_{\mathbf{S}}) \dot{\mathbf{S}}]. \quad (24)
\end{aligned}$$

It is evident that there are no nonzero real values for $\beta + \gamma$ such that $2(\beta + \gamma) - \alpha^2 = 0$ and $2(\beta + \gamma) + \alpha^2 = 0$. If we choose $\alpha = \varepsilon + \omega = 2\omega$ and $2(\beta + \gamma) = \alpha^2$, which is one of the best possibilities of reducing absolute magnitudes of $E^{(2)}$ including the velocity Verlet⁸⁸ equivalent ($\alpha = 1$, $\beta = \varepsilon = \omega = 1/2$, and $\gamma = 0$) in GCs, then the $E(\Delta t)$ is found to be

$$E(\Delta t) = E(0) + \frac{\Delta t^2}{2} \alpha^2 \{ \dot{\mathbf{S}}^T [(\ddot{\mathbf{S}}^T \partial_{\mathbf{S}}) \mathbf{g}] \dot{\mathbf{S}} \} (0) + O(\Delta t^3). \quad (25)$$

Different from this, our recent analysis for the corresponding CCMD scheme showed that in terms of CCs the total energy is expanded by⁸⁴

$$\begin{aligned}
E(\Delta t) = & E(0) + \frac{\Delta t^3}{12} \{ 3\alpha(4\gamma + \alpha^2) \ddot{\mathbf{X}}^T (\partial_{\mathbf{X}}^2 V_c) \dot{\mathbf{X}} \\
& - \alpha^3 \dot{\mathbf{X}}^T [(\dot{\mathbf{X}}^T \partial_{\mathbf{X}}) (\partial_{\mathbf{X}}^2 V_c)] \dot{\mathbf{X}} \} (0) + O(\Delta t^4). \quad (26)
\end{aligned}$$

Therefore, it is clear that, when $\partial_{\mathbf{S}} \mathbf{g} \neq \mathbf{0}$, the general ICMD scheme generates a local error in energy during each time step that is one-order larger in Δt than that resulting from the CCMD scheme. The Δt^2 -dependence of the leading local error in terms of GCs as given by eq. (25) is consistent with the result in terms

of the Riemannian coordinates of Gibson and Scheraga.⁵² Note that if $\mathbf{S} = \mathbf{X}$ then $\partial_{\mathbf{S}} \mathbf{g} = \partial_{\mathbf{X}} \mathbf{m} = \mathbf{0}$ resulting in $E^{(2)} = 0$. Thus, the very term $\partial_{\mathbf{S}} \mathbf{g}$, which causes the equations of motion to be nonlinear if it is nonzero, enforces the dynamics integration scheme in GCs to be less stable than that in CCs. This theoretical analysis is consistent with the simulation results for a system of an isolated octane molecule, the details being presented in Application to an *n*-Octane Molecule.

ICMD Algorithms

Dynamics trajectory information in GCs requires computing $\ddot{\mathbf{S}}$ at each integration time step. As shown in eq. (14), this involves computing either \mathbf{A}_2 or \mathbf{B}_2 . Since calculation of \mathbf{A}_2 is nontrivial and requires larger storage than that of \mathbf{B}_2 , we have investigated dynamics processes using \mathbf{B}_2 . In the presence of the internal constraints of eq. (6), however, we additionally need to determine $\mathbf{\Lambda}$ either by solving eq. (11) or in another way. We label any unconstrained and constrained quantities in GCs by “u” and “c”, respectively. Two ICMD schemes further refined from our early B-matrix ICMD method^{82,83} are presented later.

Algorithm AICMD

This integration scheme updates positions and velocities in GCs. Since, in the presence of internal constraints, we can determine values of $\dot{\mathbf{S}}_u(\Delta t)$ only after knowing values of $\ddot{\mathbf{S}}(\Delta t)$ [see eq. (16)], we initially approximate $\dot{\mathbf{S}}_u(\Delta t)$ by

$$\dot{\mathbf{R}}_u(\Delta t) = \dot{\mathbf{S}}_u(0) + \Delta t \ddot{\mathbf{S}}_u(0). \quad (27)$$

From this, $\dot{\mathbf{S}}_u(\Delta t)$ and $\ddot{\mathbf{S}}_u(\Delta t)$ are iteratively adjusted to follow the velocity Verlet equivalent with

$$\dot{\mathbf{w}}_u(\Delta t) \equiv \dot{\mathbf{S}}_u(0) + \frac{\Delta t}{2} \ddot{\mathbf{S}}_u(0). \quad (28)$$

The AICMD procedures are summarized as follows:

- Compute $\mathbf{A}(k)$, $\mathbf{B}(k)$, $\mathbf{B}_2(k)$, and $\mathbf{F}_X(k) \equiv -\partial_{\mathbf{X}(k)} V$.
- Set initial atomic velocities: $\dot{\mathbf{X}}(k) \equiv \mathbf{A}_u(k) \dot{\mathbf{R}}_u(k)$.
- Iterate for $\dot{\mathbf{S}}_u(k)$ and $\ddot{\mathbf{S}}_u(k)$:
 - Solve $\mathbf{G}_{cc} \mathbf{\Lambda}(k) = \mathbf{B}_c(k) \mathbf{m}^{-1} \mathbf{F}_X(k) + \dot{\mathbf{X}}^T(k) \mathbf{B}_{2c}(k) \dot{\mathbf{X}}(k)$ for $\mathbf{\Lambda}(k)$.
 - Obtain CC accelerations: $\ddot{\mathbf{X}}(k) = \mathbf{m}^{-1} \mathbf{F}_X(k) - \mathbf{m}^{-1} \mathbf{B}_c^T(k) \mathbf{\Lambda}(k)$.
 - Obtain GC accelerations: $\ddot{\mathbf{S}}_u(k) = \mathbf{B}_u \ddot{\mathbf{X}}(k) + \dot{\mathbf{X}}^T(k) \mathbf{B}_{2u}(k) \dot{\mathbf{X}}(k)$.
 - Set $\dot{\mathbf{S}}_u(k) = \dot{\mathbf{w}}_u(k) + \Delta t \ddot{\mathbf{S}}_u(k)/2$ [velocity Verlet equivalent in GCs].
 - Set $\dot{\mathbf{X}}(k) = \mathbf{A}_u(k) \dot{\mathbf{S}}_u(k)$ and go to (1).
- Set $\dot{\mathbf{w}}_u(k+1) \equiv \dot{\mathbf{S}}_u(k) + \Delta t \ddot{\mathbf{S}}_u(k)/2$ and $\dot{\mathbf{R}}_u(k+1) \equiv \dot{\mathbf{S}}_u(k) + \Delta t \dot{\mathbf{S}}_u(k)$.
- Set new GC values: $\mathbf{S}_u(k+1) = \mathbf{S}_u(k) + \Delta t \dot{\mathbf{w}}_u(k+1)$.
- Compute $\mathbf{X}(k+1)$ from $\mathbf{S}(k+1)$.
- Go to (a) with $k = k + 1$.

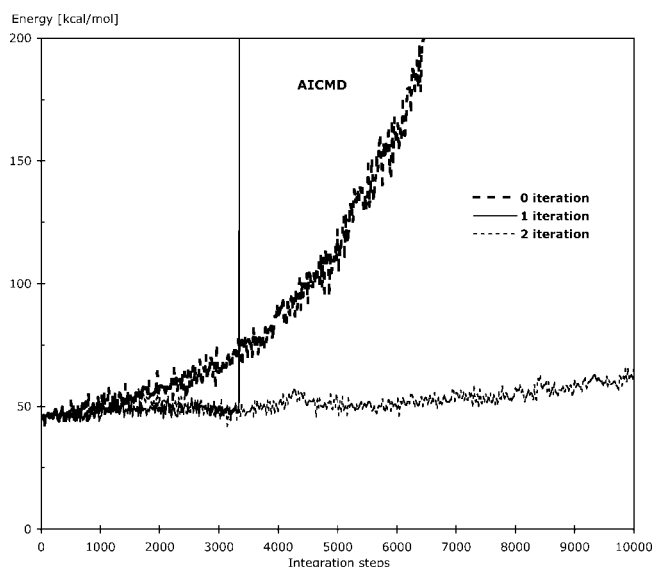


Figure 1. Energy ($T + V$) versus integration steps for constrained AICMD simulations with $\Delta t = 2$ fs, and 0, 1, and 2 iterations of GC velocities [see AICMD scheme]. The 1-iteration curve ends with the spike.

For given atomic velocities in GCs, the constrained atomic velocities in CCs are obtained by step (b). The computation cost involved in the iteration of step (c) is negligible compared to that of calculating \mathbf{F}_X . With zero iteration meaning no return from (c5) to step (c1), in most cases two iterations are enough to reach a convergence in $\dot{\mathbf{S}}_u$ that maintains stable energies (Fig. 1).

When there is no constraint, we skip the linear equation solving of (c1) and atomic accelerations are simply given by $\ddot{\mathbf{X}} = \mathbf{m}^{-1}\mathbf{F}_X$.

Algorithm BICMD

When GC accelerations are determined by the last expression of eq. (14), computing $\dot{\mathbf{X}}$ and $\ddot{\mathbf{X}}$ are required at each time step. Thus, in this scheme, atomic velocities are updated in CCs and positions are updated in GCs at each integration time step.⁸⁵ With internal constraints of eq. (6), the desired atomic velocities and accelerations in CCs can be efficiently determined in the same way as in WIGGLE.⁸⁴ By defining

$$\dot{\mathbf{q}}(\Delta t) \equiv \frac{1}{\Delta t} \{\mathbf{X}(\Delta t) - \mathbf{X}(0)\}, \quad (29)$$

the BICMD scheme is specifically outlined as follows:

- Compute $\mathbf{B}(k)$, $\mathbf{B}_2(k)$, and $\mathbf{F}_X(k) \equiv -\partial_{\mathbf{X}(k)}V$.
- Set initial atomic velocities: $\dot{\mathbf{Z}}(k) = \dot{\mathbf{q}}(k) + \Delta t \mathbf{m}^{-1}\mathbf{F}_X(k)/2$.
- Adjust $\dot{\mathbf{X}}(k)$ from the $\dot{\mathbf{Z}}(k)$ so that $\mathbf{B}_c(k)\dot{\mathbf{X}}(k) = \mathbf{0}$:
 - Solve $\mathbf{G}_{cc}\Gamma(k) = \mathbf{B}_c(k)\Gamma(k)$ for $\Gamma(k)$.
 - Compute desired velocities: $\dot{\mathbf{X}}(k) = \dot{\mathbf{Z}}(k) - \mathbf{m}^{-1}\mathbf{B}_c^T(k)\Gamma(k)$.
- Set CC accelerations: $\ddot{\mathbf{X}}(k) = 2\{\dot{\mathbf{X}}(k) - \dot{\mathbf{q}}(k)\}/\Delta t$ [velocity Verlet].
- Obtain $\dot{\mathbf{S}}_u(k) = \mathbf{B}_u\dot{\mathbf{X}}(k)$ and $\ddot{\mathbf{S}}_u(k) = \mathbf{B}_u\ddot{\mathbf{X}}(k) + \dot{\mathbf{X}}^T(k)\mathbf{B}_{2u}\dot{\mathbf{X}}(k)$.

- Set new GC values: $\mathbf{S}_u(k+1) = \mathbf{S}_u(k) + \Delta t\{\dot{\mathbf{S}}_u(k) + \Delta t\ddot{\mathbf{S}}_u(k)/2\}$.
- Compute $\mathbf{X}(k+1)$ from $\mathbf{S}(k+1)$.
- Set $\dot{\mathbf{q}}(k+1) = \frac{1}{\Delta t}\{\mathbf{X}(k+1) - \mathbf{X}(k)\}$.
- Go to (a) with $k = k+1$.

At each time step, the above process requires adjusting $\dot{\mathbf{X}}$ so as to satisfy the hidden constraints [eq. (9)], which can be expedited by the WIGGLE method.⁸⁴ For more accurate $\ddot{\mathbf{X}}(k)$ with an additional linear equation solving, step (d) can be replaced by d. Obtain atomic accelerations:

- Solve $\mathbf{G}_{cc}\Lambda(k) = \mathbf{B}_c(k)\mathbf{m}^{-1}\mathbf{F}_X(k) + \dot{\mathbf{X}}^T(k)\mathbf{B}_{2c}(k)\dot{\mathbf{X}}(k)$ for $\Lambda(k)$.
- Compute CC accelerations: $\ddot{\mathbf{X}}(k) = \mathbf{m}^{-1}\mathbf{F}_X(k) - \mathbf{m}^{-1}\mathbf{B}_c^T(k)\Lambda(k)$.

For the corresponding unconstrained dynamics scheme, steps (c), (d), and (h) are replaced by

$$\dot{\mathbf{X}}(k) = \dot{\mathbf{q}}(k) + \frac{\Delta t}{2}\ddot{\mathbf{X}}(k) \quad (30)$$

$$\dot{\mathbf{q}}(k+1) = \dot{\mathbf{X}}(k) + \frac{\Delta t}{2}\ddot{\mathbf{X}}(k), \quad (31)$$

with $\ddot{\mathbf{X}}(k) = \mathbf{m}^{-1}\mathbf{F}_X(k)$.

Our test of an isolated octane molecule shows that the constrained BICMD scheme slowly dissipates the system's total energy even with a small time step (Fig. 2). Such a decrease in energy disappears for unconstrained BICMD simulations.

Application to an *n*-Octane Molecule

For comparisons of dynamic characteristics between CCMD and ICMD simulations, we consider a system of an isolated *n*-octane

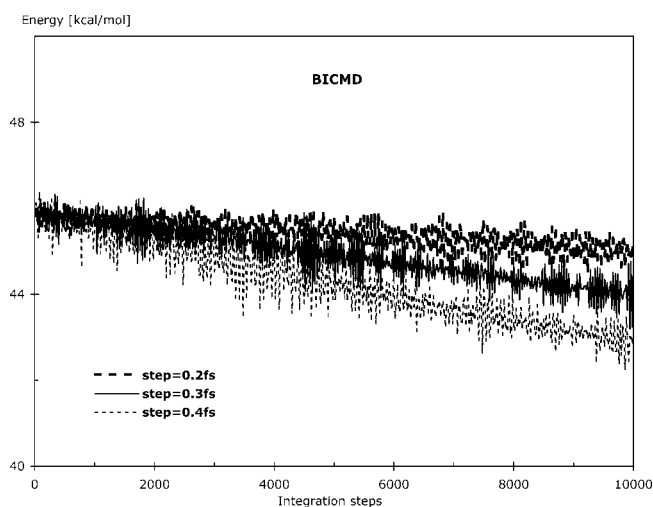


Figure 2. Energy ($T + V$) versus integration steps for constrained BICMD simulations with different Δt .

molecule. Since some C—C stretching frequencies are within the range of some angle bending frequencies, we fix only the CH bond lengths (to 1.08 Å) for constrained simulations. All the linear equations involved in these constrained dynamics simulations were solved by the conjugate gradient method. Specifically, the method was preconditioned by diagonal elements of \mathbf{G}_{cc} with a tolerance of 10^{-8} for the weighted square of the residual.⁹⁰ The constrained CCMD algorithms used for the simulation results labeled SHAKE and RATTLE differ from their original versions. Details of these modifications of the original SHAKE³⁹ and RATTLE⁴⁰ algorithms were reported in our previous paper.⁸⁴

Computations were done on a single node (512 Mbytes of memory and 1.2 GHz processing speed) of a LINUX cluster, using the SDF force field for hydrocarbon chains optimized to reproduce *ab initio* structures, energies, and vibrational frequencies.⁹¹ The system was equilibrated to provide average values of temperature and energy ($T + V$) (for 1000 steps with $\Delta t = 0.5$ fs) of 300.2 K and 45.86 kcal/mol, respectively, for constrained simulations (300 K and 42.20 kcal/mol for unconstrained simulations). The desired initial configuration had atomic velocities correspond-

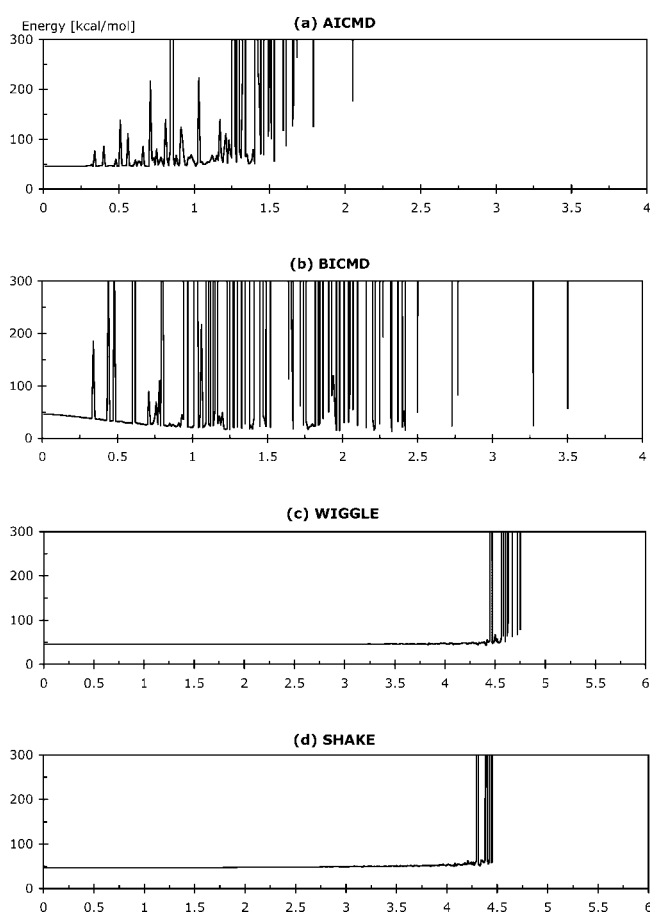


Figure 3. Energy [kcal/mol] versus time step Δt [fs] for various constrained MD simulations of an isolated *n*-octane molecule: (a) AICMD, (b) BICMD, (c) WIGGLE, and (d) SHAKE. Instantaneous energies ($T + V$) at the 50,000th integration step are shown. The time step was scanned in increments of 0.01 fs.

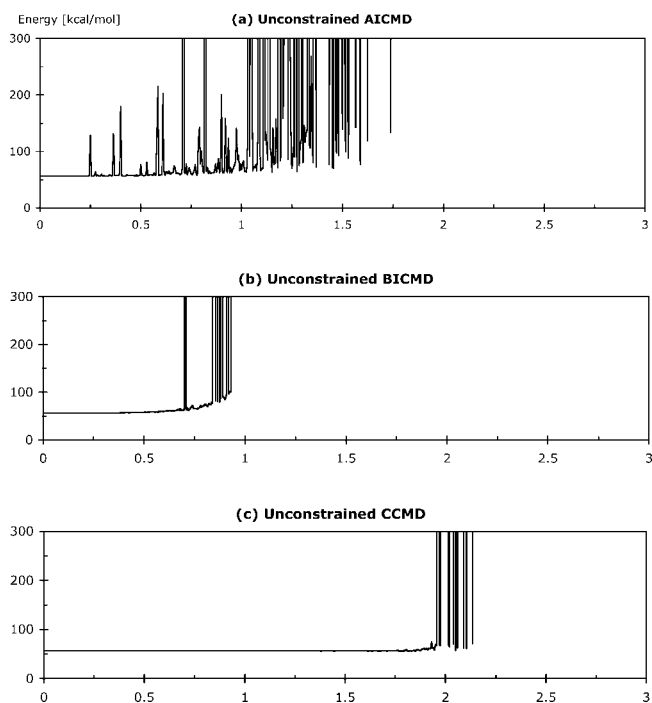


Figure 4. Total energy [kcal/mol] versus time step Δt [fs] for unconstrained MD simulations: (a) AICMD, (b) BICMD, and (c) velocity Verlet CCMD. Instantaneous energies at the 50,000th integration step are shown. The time step was scanned in increments of 0.005 fs.

ing to an instantaneous temperature of 312.9 K for constrained simulations (350.2 K for unconstrained simulations), with all backbone $\tau(\text{C—C—C—C})$ torsions having trans conformations except for the center torsion angle of 52° for both constrained and unconstrained MD simulations. The initial atomic velocities were adjusted so as to remove linear and angular momenta about the center of mass by using our previous method.⁸⁴

Although the system's total energy contains potential energy $\sigma^T \Lambda$ due to constraint forces for internal constraints, this is ignored in our figures. Stability of constrained MD simulations can also be tested by monitoring values of $T + V$. Figure 3 shows instantaneous energy ($T + V$ in kcal/mol) versus time step Δt (in fs) at the 50,000th integration step for different methods of constrained ICMD and CCMD simulations with internal constraints on all CH bond lengths. Results from unconstrained MD simulations are shown in Figure 4. It is seen that MD simulations in CCs are more stable than those in ICs, consistent with the theoretical analysis presented in Local Energy Drift. In ICMD simulations, stable regions in Δt can be extended toward an increased time step by imposing rigid constraints on all CH bond lengths, but ripples in energy, which are a direct indication of the system's instability, still exist even below 0.5 fs. The ripples in the region of a fairly small Δt , where the corresponding constrained CCMD simulations are stable, seem to arise from the nonlinearity of the equations of motion in ICs in contrast to the linearity in CCs. Constrained MD simulation results at the 100,000th integration step are shown in Figure 5. This also shows that CCMD sim-

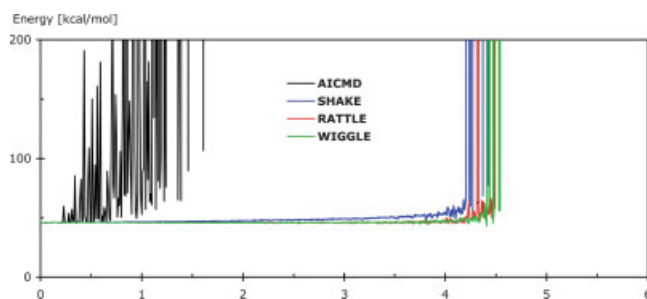


Figure 5. Energy [kcal/mol] versus time step Δt [fs] for various constrained MD simulations of an isolated *n*-octane molecule: AICMD (black), SHAKE (blue), RATTLE (red), and WIGGLE (green). Instantaneous energies ($T + V$) at the 100,000th integration step are shown. The time step was scanned in increments of 0.01 fs.

ulations are more stable than ICMD simulations, with the WIGGLE scheme being slightly better in stability than the revised SHAKE and RATTLE for constrained CCMD simulations. We have used two iteration cycles for the iteration step (c) for AICMD simulation results shown in Figures 4 and 5.

Concluding Remarks

Early MD methodology in ICs was developed for efficient analyses of conformation energy of polypeptides and proteins, and was based on torsion angles. Torsion angle MD simulations have been especially efficient in structure determinations of biomolecules by NMR spectroscopy and X-ray crystallography. Extending this work, some reports^{52,68,72,73} of stable MD simulations in torsion angles with integration time steps greater than 4 fs encouraged further improvements in ICMD methodology. This was supported by detailed studies by Mazur,^{60,86} which included all (bond length, bond angle, and torsion) ICs and concluded that there were no essential differences between ICMD and CCMD simulations. However, the situation has remained controversial, with Stocker et al, stating that "... for equilibrium simulations, Newton's equations of motion in Cartesian coordinates are to be preferred to Lagrange's equations of motion using generalized, non-Cartesian, coordinates."⁸⁷

We have made an intensive comparative study of ICMD and CCMD simulations, and obtained several results. First, for a general numerical integration scheme for ICMD simulations, we have investigated an analytic relation that provides local error in energy during an integration time step Δt . The leading local error term is found to be proportional to Δt^2 and to contain $\partial_s \mathbf{g}$, viz., the first derivative of the mass-matrix \mathbf{g} with respect to GCs [see eq. (25)]. This is an order in integration step larger than that proportional to Δt^3 for the corresponding CCMD scheme.⁸⁴ Therefore, the term $\partial_s \mathbf{g} \neq \mathbf{0}$ itself, which causes the related equations of motion to be nonlinear in GCs, is found to make ICMD simulations less stable than CCMD simulations. Second, we have introduced two ICMD schemes, AICMD and BICMD, that incorporate the second order B-matrix elements instead of the second order A-matrix elements. In the AICMD scheme, GC velocities and accelerations are iteratively adjusted so as to conform to the velocity Verlet equivalent

in GCs. In the BICMD scheme, atomic velocities with internal constraints are updated and adjusted in CCs based on the WIGGLE constrained CCMD scheme.⁸⁴ Finally, the proposed ICMD schemes have been applied to an isolated octane molecule and their performances compared with several CCMD schemes. The resulting analyses clearly show that ICMD simulations are less stable than CCMD simulations, with/without rigid constraints on all CH bond lengths. By constraining all CH bond lengths, some increased integration time steps can be found for stable ICMD simulations, but there are also some regions in Δt even smaller than 0.5 fs that generate unstable trajectories.

As far as stability is concerned, for pure MD simulations CCs are preferred to ICs, although ICs are efficient in *ab initio* geometry optimizations, MC simulations, and structural refinements for biomolecules. Any needed trajectory information in ICs can easily be obtained from that of CCMD simulations with calculated nonzero elements of B-matrices [see eqs. (1) and (14)]. As a final note, we would like to mention that dynamic trajectories are believed to be more stable for symplectic integrators than those for nonsymplectic ones in long time simulations. RATTLE has proved to be symplectic while SHAKE is not.⁹² We think it is nontrivial and beyond the scope of the present article to determine whether our presented AICMD and BICMD algorithms are symplectic or not. However, we have shown that dynamical instability in ICMD simulations will arise in any case from the nonlinearity in the equations of motion.

Acknowledgments

The authors thank Dr. Robert Krasny for many helpful discussions.

Appendix

In deriving eq. (14) from eq. (12), we have used eqs. (3) and (4), viz., the nonsingularity relations between CCs \mathbf{X} and GCs \mathbf{S} . Desired nonsingular transformation matrices \mathbf{B} , \mathbf{B}_2 , \mathbf{A} , and \mathbf{A}_2 can always be determined for a set \mathbf{S} of nonredundant GCs that is suitably chosen by combining nonredundant ICs with external rotations and translations. The calculation of nonzero elements of \mathbf{B} and \mathbf{B}_2 for external rotations has conventionally been accomplished^{1,2,93} by assuming the Casimir–Eckart conditions.^{94–96} Previously, we developed an efficient method of computing these without imposing the Casimir–Eckart conditions.⁸³ We present here a further improvement in this method.

External Rotations with Three Parameters

To compute the B-matrix elements for external rotations, we need to define a suitable molecule-fixed (MF) coordinate frame and its transformation (viz., rotation matrix) to an arbitrary laboratory-fixed (LF) coordinate frame in terms of the relative rotation angles $\vec{\phi} = (\phi^1 \phi^2 \phi^3)^T$ between the two frames. Let $\{\hat{\mathbf{1}}_{\text{MF}}, \hat{\mathbf{2}}_{\text{MF}}, \hat{\mathbf{3}}_{\text{MF}}\}$ be an arbitrary orthonormal basis for the MF frame with $\hat{\mathbf{3}}_{\text{MF}} = \hat{\mathbf{1}}_{\text{MF}} \times \hat{\mathbf{2}}_{\text{MF}}$ and any quantity in this frame being labeled by "MF." Let $\{\hat{\mathbf{1}}, \hat{\mathbf{2}}, \hat{\mathbf{3}}\}$ be the standard basis for the LF (CC) frame with $\hat{\mathbf{1}} \equiv (1 \ 0 \ 0)^T$, $\hat{\mathbf{2}} \equiv (0 \ 1 \ 0)^T$, and $\hat{\mathbf{3}} \equiv (0 \ 0 \ 1)^T$. The

position of a molecule's center-of-mass is determined only after all atomic positions are known. To expedite ICMD simulations for flexible molecules, instead of the conventional center-of-mass frame, we adopt an MF frame whose origin is located at a particular atom center \mathbf{x}_ζ . A basis for the MF frame can easily be found from any three nonlinear atomic positions including the origin atom ζ . Without a loss of generality,⁹³ we define the transformation matrix between the two frames by⁹³

$$\Xi(\vec{\phi}) \equiv \exp(\phi^3 \mathbf{D}_3) \exp(\phi^2 \mathbf{D}_2) \exp(\phi^1 \mathbf{D}_1) \\ = \begin{pmatrix} c_3 c_2 & c_3 s_2 s_1 - s_3 c_1 & c_3 s_2 c_1 + s_3 s_1 \\ s_3 c_2 & s_3 s_2 s_1 + c_3 c_1 & s_3 s_2 c_1 - c_3 s_1 \\ -s_2 & c_2 s_1 & c_2 c_1 \end{pmatrix} \quad (\text{A1})$$

with $c_j \equiv \cos \phi^j$, $s_j \equiv \sin \phi^j$, and

$$\mathbf{D}_1 \equiv \begin{pmatrix} 0 & 0 & 0 \\ 0 & 0 & -1 \\ 0 & 1 & 0 \end{pmatrix}, \mathbf{D}_2 \equiv \begin{pmatrix} 0 & 0 & 1 \\ 0 & 0 & 0 \\ -1 & 0 & 0 \end{pmatrix}, \\ \mathbf{D}_3 \equiv \begin{pmatrix} 0 & -1 & 0 \\ 1 & 0 & 0 \\ 0 & 0 & 0 \end{pmatrix}. \quad (\text{A2})$$

Then, atomic coordinates in the LF frame are related to that in MF frame by

$$\mathbf{x}_\lambda = \Xi(\vec{\phi}) \mathbf{x}_{\lambda \text{MF}} + \mathbf{x}_\zeta. \quad (\text{A3})$$

To be more specific in defining a basis for the MF frame, let atom i_1 , atom i_2 , and atom i_3 be such nonlinear atoms as shown in Figure 6, with one of these being the origin of the MF frame. Defining $\mathbf{x}_{21} \equiv \mathbf{x}_{i_1} - \mathbf{x}_{i_2}$, $\mathbf{x}_{23} \equiv \mathbf{x}_{i_3} - \mathbf{x}_{i_2}$, $\mathbf{r}_{21} \equiv |\mathbf{x}_{21}|$, $\mathbf{r}_{23} \equiv |\mathbf{x}_{23}|$, $\mathbf{e}_{21} \equiv \mathbf{x}_{21}/r_{21}$, $\mathbf{e}_{23} \equiv \mathbf{x}_{23}/r_{23}$, and $\cos \varphi_{13} \equiv \mathbf{e}_{21} \cdot \mathbf{e}_{23}$, we obtain an orthonormal vector set $\{\mathbf{e}_{21}, \mathbf{u} \equiv \mathbf{e}_{21} \times \mathbf{e}_{23} / \sin \varphi_{13}, \mathbf{v} \equiv \mathbf{u} \times \mathbf{e}_{21}\}$ in the LF frame. In view of eq. (A3), the corresponding vectors in the MF frame should satisfy

$$\{\mathbf{e}_{21}, \mathbf{v}, \mathbf{u}\} = \Xi(\vec{\phi}) \{\mathbf{e}_{21 \text{MF}}, \mathbf{v}_{\text{MF}}, \mathbf{u}_{\text{MF}}\}. \quad (\text{A4})$$

Then a desired orthonormal basis for the MF frame can be chosen so as to satisfy

$$\mathbf{e}_{21 \text{MF}} \equiv n_1 \hat{\mathbf{1}}_{\text{MF}} = (n_1 \quad 0 \quad 0)_{\text{MF}}^T \quad (\text{A5})$$

$$\mathbf{v}_{\text{MF}} \equiv n_2 \hat{\mathbf{2}}_{\text{MF}} = (0 \quad n_2 \quad 0)_{\text{MF}}^T \quad (\text{A6})$$

$$\mathbf{u}_{\text{MF}} \equiv n_3 \hat{\mathbf{3}}_{\text{MF}} = (0 \quad 0 \quad n_3)_{\text{MF}}^T \quad (\text{A7})$$

with

$$n_1 n_1 = 1 = n_2 n_2 = n_3 n_3 \quad (\text{A8})$$

$$n_1 n_2 n_3 = 1. \quad (\text{A9})$$

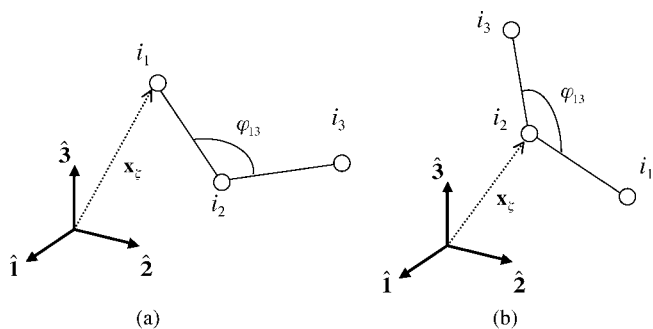


Figure 6. Definition of molecule fixed (MF) coordinate frames with three nonlinear atoms containing the origin atom ζ : (a) for $(n_1, n_2, n_3) = (-1, 1, -1)$ and (b) for $(n_1, n_2, n_3) = (1, 1, 1)$.

Relations (A8) and (A9) are simply conditions for normalization and a proper orientation, respectively. When a suitable MF frame is specifically chosen, the values of (n_1, n_2, n_3) are also fixed. For example, these can be taken as $(-1, 1, -1)$ and $(1, 1, 1)$ for the cases of Figure 6a and 6b, respectively. For our simulation results in Application to an *n*-Octane Molecule, we have used an MF frame as Figure 6a. Physical properties derived from MD trajectories are independent on the choice of an MF frame. By substituting eqs. (A5)–(A7) into (A4), equations for $\vec{\phi}$ are found to be

$$s_2 = -n_1 e_{21}^3 \quad (\text{A10})$$

$$c_1 = n_3 u^3 / c_2, \quad s_1 = n_2 v^3 / c_2 \quad (\text{A11})$$

$$c_3 = n_1 e_{21}^1 / c_2, \quad s_3 = n_1 e_{21}^2 / c_2. \quad (\text{A12})$$

Thus, from eq. (A10) ϕ^2 can be first determined within the range of $-\pi/2 < \phi^2 < \pi/2$, and next ϕ^1 and ϕ^3 are determined from eqs. (A11) and (A12), respectively. The corresponding B-matrix elements, viz., $\phi_{\lambda^k}^1 \equiv \partial \phi^1 / \partial x_\lambda^k$ or $\phi_{\nu \lambda^k}^1 \equiv \partial^2 \phi^1 / \partial x_\nu^j \partial x_\lambda^k$, can be computed by directly differentiating eqs. (A10)–(A12) with respect to atomic coordinates \mathbf{x}_λ or \mathbf{x}_ν , which are nonzero at most for $\lambda, \nu = i_1, i_2$, and i_3 .

Another direct way of computing B-matrix elements for external rotation can be found from the first derivative of eq. (A4) with respect to atomic coordinates⁸³:

$$\left\{ \frac{\partial \mathbf{e}_{12}}{\partial x_\lambda^k}, \frac{\partial \mathbf{v}}{\partial x_\lambda^k}, \frac{\partial \mathbf{u}}{\partial x_\lambda^k} \right\} = \vec{\theta}_{\lambda^k} \times \{\mathbf{e}_{12}, \mathbf{v}, \mathbf{u}\} \quad (\text{A13})$$

with $\vec{\theta}_{\lambda^k} \equiv \partial \vec{\theta} / \partial x_\lambda^k$ being related to $\phi_{\lambda^k}^1$ by the transformation of

$$\begin{pmatrix} \theta_{\lambda^k}^1 \\ \theta_{\lambda^k}^2 \\ \theta_{\lambda^k}^3 \end{pmatrix} \equiv \begin{pmatrix} c_3 c_2 & -s_3 & 0 \\ s_3 c_2 & c_3 & 0 \\ -s_2 & 0 & 1 \end{pmatrix} \begin{pmatrix} \phi_{\lambda^k}^1 \\ \phi_{\lambda^k}^2 \\ \phi_{\lambda^k}^3 \end{pmatrix} \equiv \mathbf{W}(\vec{\phi}) \begin{pmatrix} \phi_{\lambda^k}^1 \\ \phi_{\lambda^k}^2 \\ \phi_{\lambda^k}^3 \end{pmatrix}. \quad (\text{A14})$$

This defines the molecule's intrinsic angular velocity by $\vec{\Omega} \equiv \vec{\theta} \equiv \mathbf{W}(\vec{\phi}) \vec{\phi}$. In our previous report,⁸³ from the total of nine

algebraic equations of (A13) a suitable set of three independent relations was selected and solved for $\vec{\theta}_{\lambda^k}$. However, we have recently investigated a more efficient way to accomplish this. Applying inner products with \mathbf{e}_{21} , \mathbf{v} , and \mathbf{u} to both sides of eq. (A13), we obtain

$$\vec{\theta}_{\lambda^k} \cdot \mathbf{e}_{21} = \mathbf{u} \cdot \frac{\partial \mathbf{v}}{\partial x_{\lambda^k}^k}, \quad \vec{\theta}_{\lambda^k} \cdot \mathbf{v} = \mathbf{e}_{21} \cdot \frac{\partial \mathbf{u}}{\partial x_{\lambda^k}^k}, \quad \vec{\theta}_{\lambda^k} \cdot \mathbf{u} = \mathbf{v} \cdot \frac{\partial \mathbf{e}_{21}}{\partial x_{\lambda^k}^k}. \quad (\text{A15})$$

This means $\vec{\theta}_{\lambda^k}$ is expressible by

$$\vec{\theta}_{\lambda^k} = \left(\mathbf{u} \cdot \frac{\partial \mathbf{v}}{\partial x_{\lambda^k}^k} \right) \mathbf{e}_{21} + \left(\mathbf{e}_{21} \cdot \frac{\partial \mathbf{u}}{\partial x_{\lambda^k}^k} \right) \mathbf{v} + \left(\mathbf{v} \cdot \frac{\partial \mathbf{e}_{21}}{\partial x_{\lambda^k}^k} \right) \mathbf{u} \quad (\text{A16})$$

as far as $\{\mathbf{e}_{21}, \mathbf{v}, \mathbf{u}\}$ is complete and orthonormal, which is true for nonlinear \mathbf{x}_{i_1} , \mathbf{x}_{i_2} , and \mathbf{x}_{i_3} . Differentiating this with respect to x_{ν}^k and using eq. (A13), we obtain

$$\begin{aligned} \vec{\theta}_{\nu\lambda^k} &= \left[\mathbf{u} \cdot \frac{\partial^2 \mathbf{v}}{\partial x_{\nu}^k \partial x_{\lambda^k}^k} + \left(\mathbf{e}_{21} \cdot \frac{\partial \mathbf{v}}{\partial x_{\nu}^k} \right) \left(\mathbf{e}_{21} \cdot \frac{\partial \mathbf{u}}{\partial x_{\lambda^k}^k} \right) \right] \mathbf{e}_{21} \\ &+ \left[\mathbf{e}_{21} \cdot \frac{\partial^2 \mathbf{u}}{\partial x_{\nu}^k \partial x_{\lambda^k}^k} + \left(\mathbf{v} \cdot \frac{\partial \mathbf{u}}{\partial x_{\nu}^k} \right) \left(\mathbf{v} \cdot \frac{\partial \mathbf{e}_{21}}{\partial x_{\lambda^k}^k} \right) \right] \mathbf{v} \\ &+ \left[\mathbf{v} \cdot \frac{\partial^2 \mathbf{e}_{21}}{\partial x_{\nu}^k \partial x_{\lambda^k}^k} + \left(\mathbf{u} \cdot \frac{\partial \mathbf{e}_{21}}{\partial x_{\nu}^k} \right) \left(\mathbf{u} \cdot \frac{\partial \mathbf{v}}{\partial x_{\lambda^k}^k} \right) \right] \mathbf{u} \quad (\text{A17}) \end{aligned}$$

with $\vec{\theta}_{\nu\lambda^k} \equiv \partial^2 \vec{\theta} / \partial x_{\nu}^k \partial x_{\lambda^k}^k$. From eq. (A14), B-matrix elements for external rotations are now obtained by

$$\vec{\phi}_{\lambda^k} = \mathbf{W}^{-1} \vec{\theta}_{\lambda^k} \quad (\text{A18})$$

$$\vec{\phi}_{\nu\lambda^k} = \mathbf{W}^{-1} \left(\vec{\theta}_{\nu\lambda^k} - \left[\frac{\partial \mathbf{W}}{\partial x_{\nu}^k} \right] \vec{\phi}_{\lambda^k} \right). \quad (\text{A19})$$

In general, it is true that $\vec{\phi}_{\nu\lambda^k} = \vec{\phi}_{\lambda^k\nu}$, while we may have $\vec{\theta}_{\nu\lambda^k} \neq \vec{\theta}_{\lambda^k\nu}$.

For computational efficiency, instead of directly applying eqs. (A16) to (A18), we consider the values of $\vec{\theta}_{\lambda^k}$ in the MF frame, which from eqs. (A5) to (A7) are given by

$$\vec{\theta}_{\lambda^k\text{MF}} \equiv \Xi^{-1} \vec{\theta}_{\lambda^k} = \left(n_1 \mathbf{u} \cdot \frac{\partial \mathbf{v}}{\partial x_{\lambda^k}^k} \quad n_2 \mathbf{e}_{21} \cdot \frac{\partial \mathbf{u}}{\partial x_{\lambda^k}^k} \quad n_3 \mathbf{v} \cdot \frac{\partial \mathbf{e}_{21}}{\partial x_{\lambda^k}^k} \right)_{\text{MF}}^T. \quad (\text{A20})$$

Then, the expression for $\vec{\phi}_{\lambda^k}$ is simplified as

$$\begin{aligned} \vec{\phi}_{\lambda^k} &= \mathbf{W}^{-1} \mathbf{Z} \mathbf{Z}^{-1} \vec{\theta}_{\lambda^k} = \mathbf{W}^{-1} \mathbf{Z} \vec{\theta}_{\lambda^k\text{MF}} \\ &= (\theta_{\lambda^k\text{MF}}^1 + s_2 \tau_{\lambda^k} / c_2 \quad c_1 \theta_{\lambda^k\text{MF}}^2 - s_1 \theta_{\lambda^k\text{MF}}^3 \quad \tau_{\lambda^k} / c_2)^T \quad (\text{A21}) \end{aligned}$$

with

$$\tau_{\lambda^k} \equiv s_1 \theta_{\lambda^k\text{MF}}^2 + c_1 \theta_{\lambda^k\text{MF}}^3. \quad (\text{A22})$$

Next, we consider the fact that the involved derivatives with respect to the three atomic positions \mathbf{x}_{i_1} , \mathbf{x}_{i_2} , and \mathbf{x}_{i_3} , can be computed from derivatives with respect to the two bond vectors $\mathbf{a} \equiv \mathbf{x}_{21}$ and $\mathbf{b} \equiv \mathbf{x}_{23}$ such as

$$\partial \vec{\phi} / \partial x_{i_1}^k = \vec{\phi}_{a^k}, \quad \partial \vec{\phi} / \partial x_{i_2}^k = -\vec{\phi}_{a^k} - \vec{\phi}_{b^k}, \quad \partial \vec{\phi} / \partial x_{i_3}^k = \vec{\phi}_{b^k}. \quad (\text{A23})$$

Thus, eq. (A21) for the first order B-matrix elements splits into

$$\vec{\phi}_{a^k} = \left(\theta_{a^k\text{MF}}^1 + \frac{s_2}{c_2} \tau_{a^k} \quad c_1 \theta_{a^k\text{MF}}^2 - s_1 \theta_{a^k\text{MF}}^3 \quad \frac{1}{c_2} \tau_{a^k} \right)^T \quad (\text{A24})$$

$$\vec{\phi}_{b^k} = \left(\theta_{b^k\text{MF}}^1 \quad 0 \quad 0 \right)^T. \quad (\text{A25})$$

Elements in the right-hand side of these can be efficiently computed by

$$\vec{\theta}_{a^k\text{MF}} = \frac{1}{r_{21}} \left(-n_1 \frac{\cos \varphi_{13}}{\sin \varphi_{13}} u^k \quad -n_2 u^k \quad n_3 v^k \right)_{\text{MF}}^T \quad (\text{A26})$$

$$\vec{\theta}_{b^k\text{MF}} = \frac{1}{r_{23}} \left(\frac{n_1}{\sin \varphi_{13}} u^k \quad 0 \quad 0 \right)_{\text{MF}}^T \quad (\text{A27})$$

$$\tau_{\mathbf{a}} = (\tau_{a^1} \quad \tau_{a^2} \quad \tau_{a^3})_{\text{MF}}^T = \frac{1}{r_{21}} (-n_1 s_3 \quad n_1 c_3 \quad 0)_{\text{MF}}^T \quad (\text{A28})$$

$$\tau_{\mathbf{b}} = (\tau_{b^1} \quad \tau_{b^2} \quad \tau_{b^3})_{\text{MF}}^T = \mathbf{0}_{\text{MF}}, \quad (\text{A29})$$

with

$$\mathbf{u}_{a^k} \equiv \frac{\partial \mathbf{u}}{\partial a^k} = \frac{1}{r_{21} \sin \varphi_{13}} \{ \hat{\mathbf{k}} \times \mathbf{e}_{23} + (\mathbf{u} \times \mathbf{e}_{23})^k \mathbf{u} \} \quad (\text{A30})$$

$$\mathbf{u}_{b^k} \equiv \frac{\partial \mathbf{u}}{\partial b^k} = \frac{1}{r_{23} \sin \varphi_{13}} \{ \mathbf{e}_{21} \times \hat{\mathbf{k}} - v^k \mathbf{u} \}. \quad (\text{A31})$$

Thus, the expression for $\phi_{a^k}^2$ in eq. (A24) is further simplified as

$$\phi_{\mathbf{a}}^2 = (-s_2 \tau_{a^2} \quad s_2 \tau_{a^1} \quad -n_1 c_2 / r_{21})^T. \quad (\text{A32})$$

Expressions for higher order derivatives of \mathbf{u} with respect to the bond vectors can be found elsewhere,⁸⁹ which is useful to compute nonzero elements of \mathbf{B}_2 for the external rotations.

Similarly, all nonzero expressions for the second order derivatives of $\vec{\phi}$ with respect to the two bond vectors are listed by

$$\phi_{a^i a^k}^1 = \theta_{a^i a^k\text{MF}}^1 + \frac{s_2}{c_2} \left(\tau_{a^i a^k} + \frac{1}{s_2} \phi_{a^i}^2 \phi_{a^k}^3 \right) \quad (\text{A33})$$

$$\phi_{a'a^1}^2 = -c_2 \phi_{a'a^1}^2 \tau_{a^2} - s_2 \tau_{a'a^2} \quad (\text{A34})$$

$$\phi_{a'a^2}^2 = c_2 \phi_{a'a^2}^2 \tau_{a^1} + s_2 \tau_{a'a^1} \quad (\text{A35})$$

$$\phi_{a'a^3}^2 = -\frac{1}{r_{21}} \left(e_{21}^3 \phi_{a'a^1}^2 + e_{21}^j \phi_{a'a^3}^2 \right) \quad (\text{A36})$$

$$\phi_{a'a^k}^3 = \frac{1}{c_2} \left(\tau_{a'a^k} + s_2 \phi_{a'a^1}^2 \phi_{a'a^k}^3 \right) \quad (\text{A37})$$

$$\phi_{b'j b^k}^1 = \theta_{b'j b^k}^1 \text{MF} \quad (\text{A38})$$

$$\phi_{b'j a^k}^1 = \phi_{a^k b^j}^1 = \theta_{a^k b^j}^1 \text{MF} = \theta_{b'j a^k}^1 \text{MF}. \quad (\text{A39})$$

Here, the necessary expressions for $\vec{\theta}_{a^i a^k}^j \text{MF}$, $\vec{\theta}_{b'j b^k}^i \text{MF}$, $\vec{\theta}_{b'j a^k}^i \text{MF}$, and $\tau_{a^i a^k} \equiv \partial \tau_{a^i} / \partial a^j$ are found to be

$$\begin{aligned} \tau_{a^i a^k} &= (\tau_{a^i a^1} \quad \tau_{a^i a^2} \quad \tau_{a^i a^3})_{\text{MF}}^T \\ &= \left(-\tau_{a^2} \phi_{a^1}^3 - \frac{e_{21}^j}{r_{21}} \tau_{a^1} \quad \tau_{a^1} \phi_{a^1}^3 - \frac{e_{21}^j}{r_{21}} \tau_{a^2} \quad 0 \right)_{\text{MF}}^T \end{aligned} \quad (\text{A40})$$

$$\begin{aligned} \theta_{a^i a^k}^j \text{MF} &= \frac{-n_1}{r_{21}^2 \sin^2 \varphi_{13}} \{ v^j u^k + v^k u^j - \sin \varphi_{13} [\cos \varphi_{13} e_{21}^j u^k + e_{23}^k u^j] \} \\ &= \frac{1}{r_{21}} \left\{ n_3 v^j \theta_{a^i \text{MF}}^2 - \left(e_{21}^j - \frac{\cos \varphi_{13}}{\sin \varphi_{13}} v^j \right) \theta_{a^i \text{MF}}^1 \right. \\ &\quad \left. - \left(e_{21}^k - \frac{\cos \varphi_{13}}{\sin \varphi_{13}} v^k \right) \theta_{a^i \text{MF}}^1 \right\} \end{aligned} \quad (\text{A41})$$

$$\begin{aligned} \theta_{a^i a^k}^2 \text{MF} &= \frac{n_2}{r_{21}^2 \sin \varphi_{13}} \{ \sin \varphi_{13} e_{21}^j u^k - (\mathbf{u} \times \mathbf{e}_{23})^k u^j \} \\ &= \frac{1}{r_{21}} \{ n_3 v^k \theta_{a^i \text{MF}}^1 - e_{21}^j \theta_{a^i \text{MF}}^2 - e_{21}^k \theta_{a^i \text{MF}}^2 \} \end{aligned} \quad (\text{A42})$$

$$\begin{aligned} \theta_{a^i a^k}^3 \text{MF} &= \frac{n_3}{r_{21}^2 \sin \varphi_{13}} \{ e_{21}^j e_{23}^k - \cos \varphi_{13} \delta^{jk} \\ &\quad + (\mathbf{u} \times \mathbf{e}_{23})^j v^k - \sin \varphi_{13} [e_{21}^j v^k + e_{21}^k v^j] \} \\ &= \frac{1}{r_{21}} \{ n_2 u^k \theta_{a^i \text{MF}}^1 - e_{21}^j \theta_{a^i \text{MF}}^3 - e_{21}^k \theta_{a^i \text{MF}}^3 \} \end{aligned} \quad (\text{A43})$$

$$\begin{aligned} \theta_{b'j b^k}^1 \text{MF} &= \frac{-n_1}{r_{23}^2 \sin^2 \varphi_{13}} \{ v^j u^k + v^k u^j \} \text{ [since } \mathbf{v}_{b'j} \cdot \mathbf{u}_{b^k} = \mathbf{e}_{21} \cdot (\mathbf{u}_{b'j} \times \mathbf{u}_{b^k}) \\ &= 0] = \frac{-1}{r_{23} \sin \varphi_{13}} \{ v^j \theta_{b'j \text{MF}}^1 + v^k \theta_{b'j \text{MF}}^1 \} \end{aligned} \quad (\text{A44})$$

$$\begin{aligned} \theta_{b'j a^k}^1 \text{MF} &= \frac{n_1}{r_{21} r_{23} \sin^2 \varphi_{13}} \{ \cos \varphi_{13} [v^j u^k + v^k u^j] - \sin \varphi_{13} e_{21}^j u^k \} \\ &= \frac{1}{r_{23} \sin \varphi_{13}} \{ n_3 e_{21}^j \theta_{a^k \text{MF}}^2 - v^j \theta_{a^k \text{MF}}^1 - v^k \theta_{a^j \text{MF}}^1 \}. \end{aligned} \quad (\text{A45})$$

We have used $\mathbf{u}_{b'j} \cdot (\mathbf{u}_{a^k} \times \mathbf{e}_{21}) = 0$ and $\mathbf{v} \cdot (\mathbf{j} \times \mathbf{k}) = u^j e_{21}^k - u^k e_{21}^j$ in deriving the above equations.

These two direct methods of computing B-matrix elements for external rotations, viz., one from using eqs. (A10)–(A12) and the other given by eqs. (A24), (A25), and (A33)–(A39), are consistent with each other. We have verified the correctness of these analytical formulas up to second order by computational results of numerical differentiations of eqs. (A10)–(A12). The corresponding expressions for elements of \mathbf{A} and \mathbf{A}_2 can be found elsewhere.⁸²

External Rotations with Four Parameters

The above treatment of external rotations has a singularity problem for $\phi^2 = \pm \pi/2$ [see eqs. (A10)–(A12) or (A24)], and an artificial remedy is needed whenever this situation happens during simulation processes. As a way to avoid this problem, external rotations are also commonly represented by the Euler quaternion parameters $(e^0 e^1 e^2 e^3) = (e^0 \mathbf{e})$, with a normalization condition of

$$e^0 e^0 + \mathbf{e} \cdot \mathbf{e} = 1. \quad (\text{A46})$$

In terms of these parameters, the rotation matrix in real three dimensions is given by⁹⁷

$$\begin{aligned} \Xi(e^0, \mathbf{e}) &= \begin{pmatrix} e^0 e^0 - \mathbf{e} \cdot \mathbf{e} + 2e^1 e^1 & 2e^1 e^2 - 2e^0 e^3 & 2e^1 e^3 + 2e^0 e^2 \\ 2e^1 e^2 + 2e^0 e^3 & e^0 e^0 - \mathbf{e} \cdot \mathbf{e} + 2e^2 e^2 & 2e^2 e^3 - 2e^0 e^1 \\ 2e^1 e^3 - 2e^0 e^2 & 2e^2 e^3 + 2e^0 e^1 & e^0 e^0 - \mathbf{e} \cdot \mathbf{e} + 2e^3 e^3 \end{pmatrix}. \end{aligned} \quad (\text{A47})$$

During our simulations for an isolated octane molecule in Application to an *n*-Octane Molecule, we have used the former method and encountered no singular cases probably due to short simulation time range. We suggest using the conventional representation with three parameters for large molecules and the Euler representation with quaternion parameters for small molecules.

Considering the diagonal sum of this matrix $tr(\Xi)$ with eqs. (A4)–(A7), an expression to determine e^0 is found to be

$$4e^0 e^0 - 1 = e_{21}^1 e_{21 \text{MF}}^1 + v^2 v_{\text{MF}}^2 + v^3 v_{\text{MF}}^3 = n_1 e_{21}^1 + n_2 v^2 + n_3 u^3 \quad (\text{A48})$$

and the three parameters for \mathbf{e} can be determined from

$$4e^0e^1 = \Xi_{32} - \Xi_{23} = n_2v^3 - n_3u^2 \quad (\text{A49})$$

$$4e^0e^2 = \Xi_{13} - \Xi_{31} = n_3u^1 - n_1e_{21}^3 \quad (\text{A50})$$

$$4e^0e^3 = \Xi_{21} - \Xi_{12} = n_1e_{21}^2 - n_2v^1. \quad (\text{A51})$$

The corresponding B-matrix elements (e.g., $e_{\lambda^k}^0 \equiv \partial e^0 / \partial x_{\lambda^k}$, $\mathbf{e}_{\lambda^k} \equiv \partial \mathbf{e} / \partial x_{\lambda^k}$, $e_{\nu\lambda^k}^0 \equiv \partial^2 e^0 / \partial x_{\nu}^j \partial x_{\lambda^k}$, or $\mathbf{e}_{\nu\lambda^k} \equiv \partial^2 \mathbf{e} / \partial x_{\nu}^j \partial x_{\lambda^k}$) can be computed by either analytical or numerical differentiations of eqs. (A48)–(A51) with respect to atomic coordinates.

However, we have also investigated an alternative method similar to that presented in the previous section. Considering eq. (A47) and differentiating eq. (A4) with respect to atomic coordinates, we can obtain the same expression as (A13). But, in this case, the intrinsic angular momentum $\vec{\theta}$ is defined so that⁸²

$$\begin{pmatrix} 0 \\ \vec{\theta}_{\lambda^k} \end{pmatrix} = \mathbf{W} \begin{pmatrix} e_{\lambda^k}^0 \\ \mathbf{e}_{\lambda^k} \end{pmatrix} \equiv 2 \begin{pmatrix} e^0 & e^1 & e^2 & e^3 \\ -e^1 & e^0 & -e^3 & e^2 \\ -e^2 & e^3 & e^0 & -e^1 \\ -e^3 & -e^2 & e^1 & e^0 \end{pmatrix} \begin{pmatrix} e_{\lambda^k}^0 \\ e_{\lambda^k}^1 \\ e_{\lambda^k}^2 \\ e_{\lambda^k}^3 \end{pmatrix}. \quad (\text{A52})$$

The desired first order B-matrix elements can be efficiently computed by

$$\begin{aligned} \begin{pmatrix} e_{\lambda^k}^0 \\ \mathbf{e}_{\lambda^k} \end{pmatrix} &= \mathbf{W}^{-1} \begin{pmatrix} 1 & 0 \\ 0 & \Xi \end{pmatrix} \begin{pmatrix} 1 & 0 \\ 0 & \Xi^{-1} \end{pmatrix} \begin{pmatrix} 0 \\ \vec{\theta}_{\lambda^k} \end{pmatrix} \\ &= \frac{1}{2} \begin{pmatrix} e^0 & -e^1 & -e^2 & -e^3 \\ e^1 & e^0 & -e^3 & e^2 \\ e^2 & e^3 & e^0 & -e^1 \\ e^3 & -e^2 & e^1 & e^0 \end{pmatrix} \begin{pmatrix} 0 \\ \theta_{\lambda^k, \text{MF}}^1 \\ \theta_{\lambda^k, \text{MF}}^2 \\ \theta_{\lambda^k, \text{MF}}^3 \end{pmatrix} \\ &= \frac{1}{2} \begin{pmatrix} -\mathbf{e}_{\lambda^k, \text{MF}} \vec{\theta}_{\lambda^k, \text{MF}} \\ e^0 \vec{\theta}_{\lambda^k, \text{MF}} + \mathbf{e} \times \vec{\theta}_{\lambda^k, \text{MF}} \end{pmatrix}. \quad (\text{A53}) \end{aligned}$$

By differentiating this with respect to atomic coordinates x_{ν}^j , expressions for the second order B-matrix elements are found to be

$$4e_{\nu\lambda^k}^0 = -(\vec{\theta}_{\nu, \text{MF}} \cdot \vec{\theta}_{\lambda^k, \text{MF}})e^0 - \mathbf{e} \cdot (2\vec{\theta}_{\nu, \lambda^k, \text{MF}} + \vec{\theta}_{\nu, \text{MF}} \times \vec{\theta}_{\lambda^k, \text{MF}}) \quad (\text{A54})$$

$$4\mathbf{e}_{\nu\lambda^k} = -(\vec{\theta}_{\nu, \text{MF}} \cdot \vec{\theta}_{\lambda^k, \text{MF}})\mathbf{e} + e^0(2\vec{\theta}_{\nu, \lambda^k, \text{MF}} + \vec{\theta}_{\nu, \text{MF}} \times \vec{\theta}_{\lambda^k, \text{MF}}) + \mathbf{e} \times (2\vec{\theta}_{\nu, \lambda^k, \text{MF}} + \vec{\theta}_{\nu, \text{MF}} \times \vec{\theta}_{\lambda^k, \text{MF}}). \quad (\text{A55})$$

With eqs. (A26), (A27), and (A41)–(A45), the whole computation processes can also be facilitated by the derivatives with respect to the two bond vectors $\mathbf{a} = \mathbf{x}_{21}$ and $\mathbf{b} = \mathbf{x}_{23}$. Finally, the corresponding expressions for elements of \mathbf{A} and \mathbf{A}_2 can be found elsewhere.⁸²

References

- Wilson E. B., Jr.; Decius, J. C.; Cross, P. C. *Molecular Vibrations*; McGraw-Hill: New York, 1955.
- Califano, S. *Vibrational States*; Wiley: New York, 1976.
- Krimm, S.; Bandekar, J. *Adv Protein Chem* 1986, 38, 181.
- Ramachandran, G. N.; Sasisekharan, V. *Adv Protein Chem* 1968, 23, 283.
- Burkert, U.; Allinger, N. L. In *ACS Monograph 177*; Caserio, M. C., Ed.; American Chemical Society: Washington, DC, 1982.
- Némethy, G.; Gibson, K. D.; Palmer, K. A.; Yoon, C. N.; Paterlini, G.; Zagari, A.; Rumsey, S.; Scheraga, H. A. *J Phys Chem* 1992, 96, 6472.
- Li, Z.; Scheraga, H. A. *Proc Natl Acad Sci USA* 1987, 84, 6611.
- Chang, G.; Guida, W. C.; Still, W. C. *J Am Chem Soc* 1989, 111, 4379.
- Dodd, L. R.; Boone, T. D.; Theodorou, D. N. *Mol Phys* 1993, 78, 961.
- Gabb, H. A.; Lavery, R.; Prévost, C. *J Comput Chem* 1995, 16, 667.
- Deem, M. W.; Bader, J. S. *Mol Phys* 1996, 87, 1245.
- Jorgensen, W. L.; Tirado-Rives, J. *J Phys Chem* 1996, 100, 14508.
- Gabb, H. A.; Prévost, C.; Bertucat, G.; Robert, C. H.; Lavery, R. *J Comput Chem* 1997, 18, 2001.
- Dinner, A. R. *J Comput Chem* 2000, 21, 1132.
- Ulmschneider, J. P.; Jorgensen, W. L. *J Chem Phys* 2003, 118, 4261.
- Pulay, P. *Mol Phys* 1969, 17, 197.
- Schlegel, H. B. *J Comput Chem* 1982, 3, 214.
- Schlegel, H. B. *Theor Chim Acta (Berl)* 1984, 66, 333.
- Fogarasi, G.; Zhou, X.; Taylor, P. W.; Pulay, P. *J Am Chem Soc* 1992, 114, 8191.
- Pulay, P.; Fogarasi, G. *J Chem Phys* 1992, 96, 2856.
- Peng, C.; Ayala, P. Y.; Schlegel, H. B.; Frisch, M. J. *J Comput Chem* 1996, 17, 49.
- Baker, J.; Kessi, A.; Delley, B. *J Chem Phys* 1996, 105, 192.
- Baker, J. *J Comput Chem* 1997, 18, 1079.
- Paizs, B.; Fogarasi, G.; Pulay, P. *J Chem Phys* 1998, 109, 6571.
- Farkas, O.; Schlegel, H. B. *J Chem Phys* 1998, 109, 7100.
- Baker, J.; Kinghorn, D.; Pulay, P. *J Chem Phys* 1999, 110, 4986.
- Paizs, B.; Baker, J.; Suhai, S.; Pulay, P. *J Chem Phys* 2000, 113, 6566.
- Kudin, K. N.; Scuseria, G. E.; Schlegel, H. B. *J Chem Phys* 2001, 114, 2919.
- Farkas, O.; Schlegel, H. B. *J Mol Struct (Theochem)* 2003, 666/667, 31.
- Németh, K.; Challacombe, M. *J Chem Phys* 2004, 121, 2877.
- Tuzun, R. E.; Noid, D. W.; Sumpter, B. G. *J Chem Phys* 1996, 105, 5494.
- Clary, D. C. *J Chem Phys* 2001, 114, 9725.
- Abagyan, R.; Totrov, M.; Kuznetsov, D. *J Comput Chem* 1994, 15, 488.
- Totrov, M.; Abagyan, R. *Proteins* 1997, Suppl. 1, 215.
- Fernández-Recio, J.; Totrov, M.; Abagyan, R. *Protein Sci* 2002, 11, 280.
- Clare, G. M.; Schwieters, C. D. *J Am Chem Soc* 2003, 125, 2902.
- Fernández-Recio, J.; Totrov, M.; Abagyan, R. *Proteins* 2003, 52, 113.

38. Amadei, A.; Linssen, A. B. M.; Berendsen, H. J. C. *Proteins* 1993, 17, 412.
39. Ryckaert, J. P.; Ciccotti, G.; Berendsen, H. J. C. *J Comput Phys* 1977, 23, 327.
40. Andersen, H. C. *J Comput Phys* 1983, 52, 24.
41. Gö, N.; Scheraga, H. A. *J Chem Phys* 1969, 51, 4751.
42. Fixman, M.; Kovac, J. *J Chem Phys* 1974, 61, 4939.
43. Fixman, M.; Kovac, J. *J Chem Phys* 1974, 61, 4950.
44. Fixman, M. *J Chem Phys* 1978, 69, 1527.
45. Pear, M. R.; Weiner, J. H. *J Chem Phys* 1979, 71, 212.
46. Wittenburg, J. *Symposium on Dynamics of Multibody Systems (Munich, Germany, August 28–September 3, 1977)*; Magnus, K., Ed.; Springer-Verlag: Heidelberg, 1978; pp. 357.
47. Jerkovsky, W. *J Guid Cont* 1978, 1, 173.
48. Katz, H.; Walter, R.; Somorjai, R. L. *Comput Chem* 1979, 3, 25.
49. Noguti, T.; Gö, N. *J Phys Soc Japan* 1983, 52, 3283.
50. Noguti, T.; Gö, N. *J Phys Soc Japan* 1983, 52, 3685.
51. Abe, H.; Braun, W.; Noguti, T.; Gö, N. *Comput Chem* 1984, 8, 239.
52. Gibson, K. D.; Scheraga, H. A. *J Comput Chem* 1990, 11, 468.
53. Gibson, K. D.; Scheraga, H. A. *J Comput Chem* 1990, 11, 487.
54. He, S.; Scheraga, H. A. *J Chem Phys* 1998, 108, 271.
55. Bystroff, C. *Protein Eng* 2001, 14, 825.
56. Mazur, A. K.; Abagyan, R. A. *J Biomol Struct Dyn* 1989, 6, 815.
57. Abagyan, R. A.; Mazur, A. K. *J Biomol Struct Dyn* 1989, 6, 833.
58. Mazur, A. K.; Dorofeyev, V. E.; Abagyan, R. A. *J Comput Phys* 1991, 92, 261.
59. Dorofeyev, V. E.; Mazur, A. K. *J Comput Phys* 1993, 107, 359.
60. Mazur, A. K. *J Comput Chem* 1997, 11, 1354.
61. Kneller, G. R.; Hinsen, K. *Phys Rev E* 1994, 50, 1559.
62. Hinsen, K.; Kneller, G. R. *Phys Rev E* 1995, 52, 6868.
63. Bae, D.-S.; Haug, E. *J Mech Struct Mach* 1987, 15, 359.
64. Bae, D.-S.; Haug, E. *J Mech Struct Mach* 1987, 15, 481.
65. Rodriguez, G.; Jain, A.; Kreutz-Delgado, K. *Int J Rob Res* 1991, 10, 371.
66. Jain, A.; Vaidehi, N.; Rodriguez, G. *J Comput Phys* 1993, 106, 258.
67. Rice, L. M.; Brünger, A. T. *Proteins* 1994, 19, 277.
68. Mathiowetz, A. M.; Jain, A.; Karasawa, N.; Goddard W. A., III. *Proteins* 1994, 20, 227.
69. Turner, J.; Weiner, P.; Robson, B.; Venugopal, R.; Schubele H., III; Singh, R. *J Comput Chem* 1995, 16, 1271.
70. Vaidehi, N.; Jain, A.; Goddard W. A., III. *J Phys Chem* 1996, 100, 10508.
71. Stein, E. G.; Rice, L. M.; Brünger, A. T. *J Magn Reson* 1997, 124, 154.
72. Güntert, P.; Mumenthaler, C.; Wüthrich, K. *J Mol Biol* 1997, 273, 283.
73. Schwieters, C. D.; Clore, G. M. *J Magn Reson* 2001, 152, 288.
74. Rapaport, D. C. *Phys Rev E* 2002, 66, 011906.
75. Bertsch, R. A.; Vaidehi, N.; Chan, S. I.; Goddard W. A., III. *Proteins* 1998, 33, 343.
76. Klepeis, J. L.; Floudas, C. A. *Comput Chem Eng* 2000, 24, 1761.
77. Zhang, C.; Hou, J.; Kim, S.-H. *Proc Natl Acad Sci USA* 2002, 99, 3581.
78. Vaidehi, N.; Floriano, W. B.; Trabanino, R.; Hall, S. E.; Freddolino, P.; Choi, E. J.; Zamanakos, G.; Goddard W. A., III. *Proc Natl Acad Sci USA* 2002, 99, 12622.
79. Herrmann, T.; Güntert, P.; Wüthrich, K. *J Mol Biol* 2002, 319, 209.
80. Chen, J.; Im, W.; Brooks C. L., III. *J Comput Chem* 2005, 26, 1565.
81. Bardiaux, B.; Malliavin, T. E.; Nilges, M.; Mazur, A. K. *J Biomol NMR* 2006, 34, 153.
82. Lee, S.-H.; Palmo, K.; Krimm, S. *Chem Phys* 2001, 265, 63.
83. Lee, S.-H.; Palmo, K.; Krimm, S. *Chem Phys Lett* 2001, 342, 643.
84. Lee, S.-H.; Palmo, K.; Krimm, S. *J Comput Phys* 2005, 210, 171.
85. Pulay, P.; Paizs, B. *Chem Phys Lett* 2002, 353, 400.
86. Mazur, A. K. *J Phys Chem B* 1998, 102, 473.
87. Stocker, U.; Juchli, D.; van Gunsteren, W. F. *Mol Simulat* 2003, 29, 123.
88. Swope, W. C.; Andersen, H. C.; Berens, P. H.; Wilson, K. R. *J Chem Phys* 1982, 76, 637.
89. Lee, S.-H.; Palmo, K.; Krimm, S. *J Comput Chem* 1999, 20, 1067.
90. Axelsson, O. *Iterative Solution Methods*; Cambridge University Press: Cambridge, 1994.
91. Palmo, K.; Mirkin, N. G.; Krimm, S. *J Phys Chem A* 1998, 102, 6448.
92. Zhang, M. -Q.; Skeel, R. D. *J Comput Chem* 1995, 16, 365.
93. Allen, W. D.; Császár, A. G. *J Chem Phys* 1993, 98, 2983.
94. Eckart, C. *Phys Rev* 1935, 47, 552.
95. Wilson E. B., Jr.; Howard, J. B. *J Chem Phys* 1936, 4, 260.
96. Sayvetz, A. *J Chem Phys* 1939, 7, 383.
97. Evans, D. J. *Mol Phys* 1977, 34, 317.